JOURNAL OF APPLIED POLYMER SCIENCE VOL. 17, PP. 1479–1506 (1973)

Solution Polymerization of Acrylamide to High Conversion

T. ISHIGE, *Minitech Ltd., Burlington, Ontario,* and A. E. HAMIELEC, *Chemical Engineering Department, McMaster University, Hamilton, Ontario, Canada*

Synopsis

The solution polymerization of acrylamide initiated by 4,4'-azobis-4-cyanovaleric acid (ACV) at high monomer concentrations in the temperature range 25–50°C has been studied. Molecular weight distributions were measured by gel permeation chromatography and by electron microscopy. Molecular weight measurements show that transfer to monomer plays a dominant role in controlling the molecular weight averages.

INTRODUCTION

Kinetic studies of polymerization of acrylamide in water have been reported for a number of initiator systems. These include radiation initiation with x-ray, γ-ray, and UV light and chemical initiation with redox systems, peroxide, and azo compounds. Dainton and his coworkers[1–3] made a series of comprehensive studies to elucidate the reaction mechanism and to evaluate individual rate constants. It was shown that the polymerization follows typical stationary-state kinetics at low conversion and that the rate constant k_p is exceptionally large and k_t rather low as compared to other vinyl monomers.

A few kinetic studies[4–6] were made up to conversions as high as 80–90%, and these report the validity of the low-conversion kinetic scheme to high conversions, as measured conversions agreed well with predicted values. However, no measurements of molecular weight change with reaction time were made; they were measured only at final conversions. Also these high-conversion experiments were made with initial monomer concentrations less than 0.5 (mole/l.) where the molecular weight of the product polymers is of the order 10^5.

The present experimental investigation was initiated to obtain measurements of both conversion and molecular weight average with reaction time at relatively high monomer concentrations to yield polyacrylamide of number-average molecular weight greater than one million. The development of a kinetic model capable of predicting conversion and molecular weight distribution up to essentially complete conversion was another objective.

Kinetic data involving high monomer concentrations and high conversions are of special importance in industrial processes. In addition, current interest in waste water treatment with water-soluble polymers of very large molecular weights was added incentive for this investigation.

EXPERIMENTAL DETAILS AND RESULTS

Acrylamide supplied by Nalco Chemical Company (Chicago, Illinois) was twice recrystallized from chloroform. The purified acrylamide had a melting point of 84.3 ± 0.5°C. An aqueous solution of the acrylamide was analyzed for the presence of polymeric impurities by gel permeation chromatography (GPC, Waters Associates ALC Model 201). It was found that the monomer contains some polymeric impurities at less than 0.1% and that no polymerization takes place in an aqueous solution of the monomer at room temperature when kept in the dark. GPC chromatograms are shown in Figure 1 for a fresh monomer solution and the solution kept in dark for 17 days.

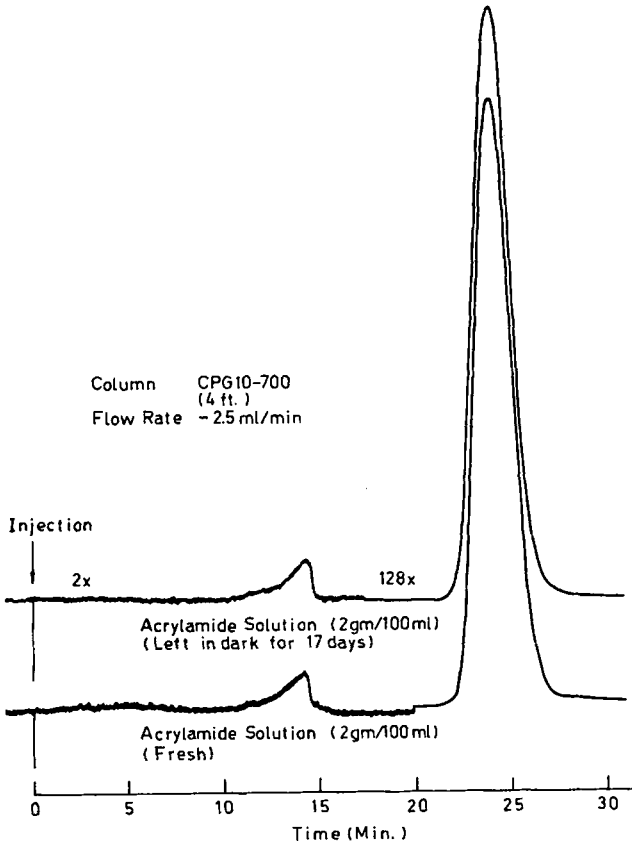

Fig. 1. GPC responses of purified acrylamide.

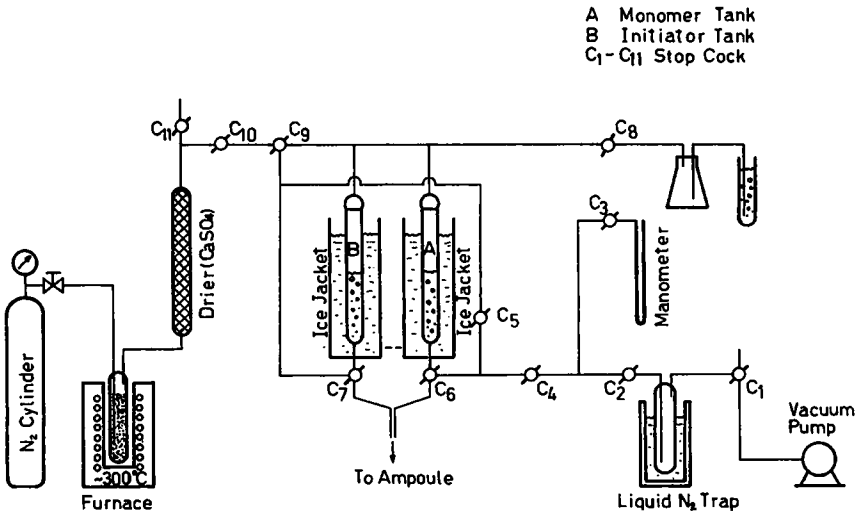

Fig. 2. Schematic diagram of deaeration apparatus.

The initiator used is 4,4′-azobis-4-cyanovaleric acid (ACV, Aldrich Chemical Company Inc.). It was purified as follows. The ACV was suspended in water at room temperature and sodium bicarbonate was added until the solid just dissolved. The solution was then acidified with HCl until it was slightly acid, causing precipitation of the ACV. The solid recovered by filtration was washed with ice-cold water. The purified ACV decomposed rapidly at 129 ± 0.5°C rather than melting.

Water used for preparing aqueous solutions of reagents and for final rinsing of reaction ampoules was triply distilled, with the final distillation made using potassium permanganate. The conductivity of this water was less than 1.2×10^{-6} mho.

The apparatus for deaeration of monomer and initiator solutions is shown in Figure 2. It consists of a vacuum line, two ice-jacketed tanks (25-ml burets) holding monomer and initiator solutions, and a nitrogen purification line. Nitrogen was introduced over heated copper wire to remove traces of oxygen, and this was used as an inert gas to deaerate the monomer and initiator solutions, and to fill the ampoule. After deaeration for 60 min by bubbling nitrogen through the two solutions, the desired amount of monomer and initiator solutions were introduced into an ampoule kept in an ice bath. Three sizes of Pyrex glass ampoules were used; O.D. 6 mm (I.D. 4 mm) × 10 cm; O.D. 12 mm (I.D. 10 mm) × 20 cm; and O.D. 15 mm (I.D. 12.5 mm) × 20 cm.

The reaction was started by transferring the ampoules into a thermostated bath. A test was made to check for prepolymerization before transferring the ampoules into the bath by breaking the ampoule and analyzing for polymer formation by GPC. The prepolymerization was found negligible. No induction period was observed, and this indicated that the deaeration period was sufficient to remove oxygen. The reaction

was quenched at a desired time by thrusting the ampoules into liquid nitrogen.

Conversion of monomer to polymer was measured either by gravimetry or by GPC. The larger two ampoules were used in the first method, and the smallest one was used in the second method. Conversion measurements by GPC were made comparing the areas under monomer and polymer peaks, and this chromatography technique enabled the rapid determination of conversion with a much smaller sample size; this then permitted the use of smaller ampoules allowing better temperature control. Calibration with known polymer fractions in monomer–polymer mixtures proved that the area fraction represents weight fractions. This is shown in Figure 3 together with an example chromatogram and area calculation by an on-line minicomputer.

The experimental runs made were of two kinds; initial rate runs and continuous high conversion runs. The initial rate runs were made to obtain reliable initial rate of polymerization, starting several ampoules at once and quenching all of them at one time near conversion of 10%. These runs were designated by the letter I. The continuous runs, designated by the first C, were made to follow the change of conversion with respect to time by quenching ampoules one after another. The reactions were followed generally to over 90% conversion. The experimental conditions of the runs are summarized in Table I.

The number-average molecular weights of precipitated polymers were calculated from measured intrinsic viscosities using an empirical relation for polydisperse polyacrylamide:

$$[\eta] = 6.80 \times 10^{-4} \bar{M}_n^{0.66}.^{1} \quad (1)$$

TABLE I
Summary of Experimental Conditions

Run no.	Temp., °C	Monomer concn., mole/l.	Initiator concn., $\times 10^4$, mole/l.
I5011, C5011(A), C5011(B) C5011(C), C5011(D)	50	0.563	1.78
I5012	50	0.563	3.56
I5014, C5014(A), C5014(B)	50	0.563	7.14
C5021(A), C5021(B)	50	1.126	1.78
I5024, C5024(A), C5024(B)	50	1.126	7.14
I5044, C5044	50	2.252	7.14
C50S(A), C50S(B)	50	0.281	7.14
I4014, C4014	40	0.563	7.14
C4024	40	1.126	7.14
C4044	40	2.252	7.14
I3014	30	0.563	7.14
I2511	25	0.563	1.78
I2512	25	0.563	3.56
I2514	25	0.563	7.14

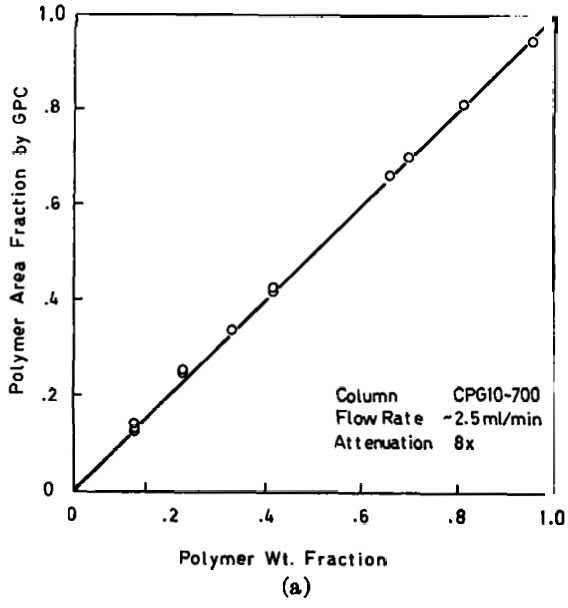

(a)

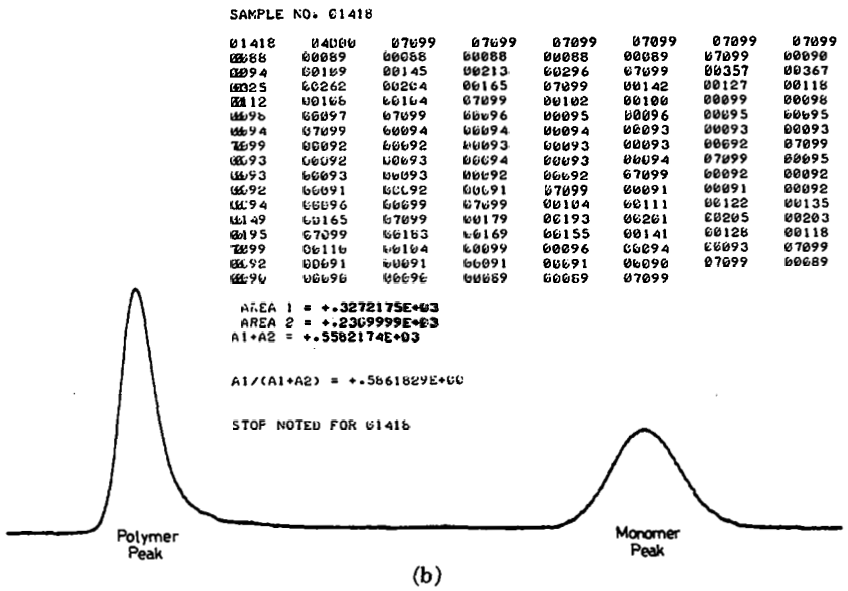

(b)

Fig. 3. (a) Comparison of weight fraction vs. peak area fraction. (b) Example of polymer and monomer response and area fraction calculation.

Additional molecular weight analyses were made using light-scattering (Brice-Phoenix Universal Light Scattering Photometer), electron microscopy (Phillips EM40), and GPC (Waters ALC 201). The experimental details are reported in Appendices I to III.

TABLE II
Summary of Initial Rate Runs

Run no.	I5011	I5012	I5014	I5024	I5044
Reaction time, min	15	12	8	8	6
Conversion (by GPC)	0.101	0.101	0.107	0.131	0.114
	0.096	0.112	0.109	0.137	0.105
	0.085	0.106	0.109	0.141	0.111
	0.090	0.116	0.112	0.119	0.115
		0.125	0.096	0.143	0.106
Average conversion	0.095	0.112	0.107	0.134	0.110
R_{p_0}[a]	5.97×10^{-5}	8.78×10^{-5}	1.25×10^{-4}	3.05×10^{-4}	6.89×10^{-4}
$f \cdot k_d$[b]	9.9×10^{-7}	1.07×10^{-6}	1.08×10^{-6}	1.57×10^{-6}	2.08×10^{-6}
	I4014	I3014	I2511	I2512	I2514
Reaction time, min	17	60	180	140	90
Conversion (by GPC)	0.079	0.117	0.100	0.099	0.101
	0.088	0.097	0.089	0.116	0.089
	0.093	0.101	0.092	0.101	0.085
	0.082	0.115	0.092	0.120	0.094
				0.122	0.103
Average conversion	0.086	0.108	0.093	0.112	0.094
R_{p_0}	4.73×10^{-5}	1.69×10^{-5}	4.85×10^{-7}	7.49×10^{-7}	9.85×10^{-6}
$f \cdot k_d$	1.8×10^{-7}	2.6×10^{-7}	9.32×10^{-9}	1.11×10^{-8}	9.6×10^{-9}

[a] R_{p_0} was calculated by $M_0 \times (\Delta x/\Delta t)$ where Δx is the average conversion and Δt is the reaction time.

[b] $f \cdot k_d$ was calculated by $R_{p_0}^2/2(k_p^2/k_t) \cdot C_0 \cdot M_0^2$.

Table II lists the measured conversions in the initial rate runs. The initial rate of polymerization R_{p_0} and the initiator (ACV) decomposition rate constant multiplied by the initiation efficiency, $f \cdot k_d$, were calculated using the averaged conversions.

Table III lists the measured conversions in the continuous runs together with predicted conversions obtained from the kinetic scheme to be described later.

Table IV lists the measured intrinsic viscosities and corresponding number-average molecular weights. Weight-average molecular weights calculated also from the intrinsic viscosities using two different empirical relations are included for comparison. The equations are as follows:

$$[\eta] = 6.31 \times 10^{-5} \bar{M}_w^{0.80,7} \tag{2}$$

$$[\eta] = 3.73 \times 10^{-5} \bar{M}_w^{0.66,8} \tag{3}$$

DATA INTERPRETATION AND COMPARISON OF MEASURED AND PREDICTED QUANTITIES

Reaction Scheme and Rate Constants

Initial rate of polymerization R_{p_0} was plotted against initial initiator and monomer concentrations (C_0, M_0) in Figures 4 and 5, respectively. The

TABLE III
Summary of Continuous Runs
Runs C5011(A), C5011(B), C5011(C), and C5011(D)

Reaction time, hr	Measured conversion (A)	(B)	(C)	(D) (all by gravimetry)	Predicted conversion
0.50	0.176	0.147	0.154	0.187 (1)	0.177
1.00	0.320 (2)	0.276	0.292	0.341 (2)	0.314
2.00		0.475 (3)	0.483 (3)	0.503	0.507
3.00	0.634 (3)	0.620	0.621	0.650 (4)	0.632
4.00	0.731	0.691	0.712		0.716
5.00	0.790 (5)		0.787	0.763	0.775
6.00	0.810 (6)		0.827		0.817
			0.854 (8)	0.860 (6)	0.849

Runs C5014(A) and C5014(B)

Reaction time, hr	Measured conversion (A) (by gravimetry)	(B) (by GPC)	Predicted conversion
0.25	0.158 (1)	0.173	0.177
0.50	0.283 (2)	0.308	0.315
1.00	0.487	0.506	0.509
1.50	0.616	0.617	0.634
2.50	0.756	0.771	0.777
3.50	0.856 (6)	0.821	0.850
5.00	0.922 (7)	0.897	0.908

Runs C5021(A) and C5021(B)

Reaction time, hr	Measured conversion (A) (both by gravimetry)	(B)	Predicted conversion
0.5	0.192 (1)	0.190	0.211
1.0	0.390	0.358	0.368
2.0	0.619 (3)	0.620	0.578
3.0	0.744	0.780	0.703
4.0	0.824 (5)	0.850	0.782
5.0	0.871	0.909	0.835
6.0	0.906 (7)	0.927	0.870

Runs C5024(A) and C5024(B)

Reaction time, hr	Measured conversion (A) (by gravimetry)	(B) (by GPC)	Predicted conversion
0.25	0.171	0.181	0.211
0.50	0.369 (2)	0.363	0.369
1.0	0.599 (3)	0.627	0.579
1.5	0.760 (4)		0.704
2.0		0.838	0.784
3.5		0.917	0.898
5.0		0.984	0.942

TABLE III (*continued*). Run C5044

Reaction time, hr	Measured conversion (by GPC)	Predicted conversion
0.25	0.220	0.238
0.50	0.423 (2)	0.412
1.0	0.694	0.634
2.0	0.903	0.834
3.0	0.953 (5)	0.911

Runs C50S(A) and C50S(B)

Reaction time, hr	Measured conversion (A) (by gravimetry)	Measured conversion (B) (by GPC)	Predicted conversion
0.25		0.135	0.142
0.50		0.250	0.257
1.00	0.435 (1)	0.447	0.429
1.50		0.550	0.550
2.50	0.697 (2)	0.708	0.700
5.00	0.850 (3)	0.873	0.861

Run C4011

Reaction time, hr	Measured conversion (by GPC)	Predicted conversion
1.0	0.172	0.153
2.0	0.292	0.276
4.0	0.451	0.457
6.5	0.612	0.604
10.0	0.718	0.731

Run C4014

Reaction time, hr	Measured conversion (by GPC)	Predicted conversion
0.5	0.163	0.154
1.0	0.274	0.277
2.0	0.483 (3)	0.458
3.0	0.600	0.581
5.0	0.735	0.731
7.0	0.810	0.809
10.0	0.881 (7)	0.883

Runs C4024(A) and C4024(B)

Reaction time, hr	Measured conversion (A) (both by GPC)	Measured conversion (B) (both by GPC)	Predicted conversion
0.5	0.172	0.160	0.185
1.0	0.298	0.325	0.329
2.0	0.524	0.562	0.529
3.0	0.725	0.720	0.657
5.0	0.877	0.863	0.799
7.0	0.914	0.909	0.870
10.0	0.955		0.923

TABLE III (*continued*) Run C4044

Reaction time, hr	Measured conversion (by GPC)	Predicted conversion
0.5	0.198	0.213
1.0	0.379 (2)	0.374
2.0	0.657 (3)	0.589
3.0	0.852	0.718
4.0	Not measured (E-1)	0.798
5.0	0.926	0.850
7.0	0.962 (6)	0.910

[a] Numbers in parentheses after conversion values designate polymer samples analyzed for molecular weight. For example, C5011(A)-2 represents the polymer obtained in the run C5011(A) at reaction time of 1 hr.

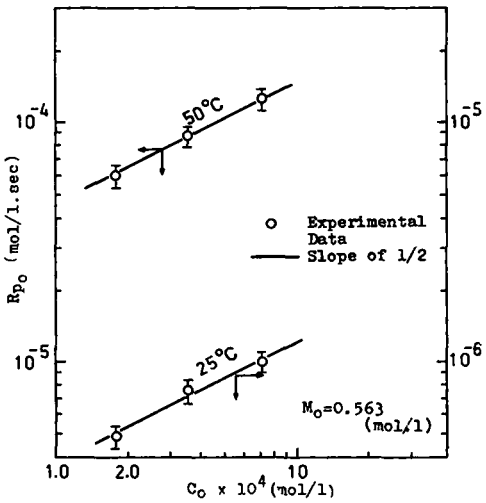

Fig. 4. Dependence of R_{p_0} on C_0.

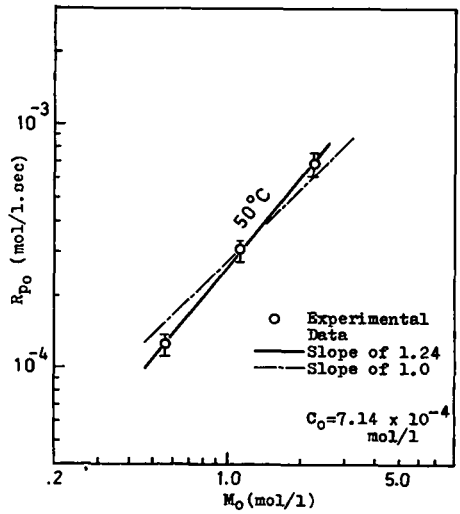

Fig. 5. Dependence of R_{p_0} on M_0.

TABLE IV. Summary of Measured Intrinsic Viscosities
Polymer Samples of Initial Rate Runs

Sample (or run no.)	Measured values				Predicted values	
	$[\eta]$	$\bar{M}_n \times 10^{-6}$ (eq. 1)	$\bar{M}_w \times 10^{-6}$ (eq. 2)	(eq. 3)	$\bar{M}_n \times 10^{-6}$	$\bar{M}_w \times 10^{-6}$
I5011	13.0	3.07	4.39	7.61	3.21	6.41
I5012	12.9	3.03	4.35	7.54	2.86	5.71
I5014	10.8	2.32	3.48	5.76	2.48	4.96
I5024	14.1	3.47	4.86	8.62	3.01	6.01
I5044	15.5	4.01	5.47	9.95	3.51	7.03
I4014	15.0	3.81	5.25	9.47	3.48	6.96
I2511	18.2	5.11	6.68	12.7	5.50	11.1
I2512	18.2	5.11	6.68	12.7	5.38	10.8
I2514	17.3	4.73	6.27	11.8	5.22	10.4

Polymer Samples of Continuous Runs

Sample code	Measured values				Predicted values	
	$[\eta]$	$\bar{M}_n \times 10^{-6}$ (eq. 1)	$\bar{M}_w \times 10^{-6}$ (eq. 2)	(eq. 3)	$\bar{M}_n \times 10^{-6}$	$\bar{M}_w \times 10^{-6}$
C5011(A)-2	15.3	3.93	5.38	9.76	3.13	6.26
C5011(A)-3	13.6	3.29	4.64	8.16	2.96	5.94
C5011(A)-5	11.9	2.68	3.93	6.67	2.86	5.76
C5011(A)-6	10.9	2.35	3.52	5.84	2.81	5.69
C5011(B)-3	13.4 ± 0.3	3.21 ± 0.11	4.56 ± 0.13	7.98 ± 0.27	3.04	6.08
C5011(C)-3	13.2 ± 0.2	3.14 ± 0.07	4.48 ± 0.08	7.80 ± 0.36	3.04	6.08
C5011(C)-8	12.4	2.86	6.3 (light scattering)		2.78	5.63
C5011(D)-1	14.6	3.66	5.07	9.09	3.18	6.36
C5011(D)-2	15.1	3.85	5.29	9.57	3.13	6.26
C5011(D)-4	12.6	2.93	4.22	7.27	2.96	5.94
C5011(D)-7	12.4	2.86	4.14	7.10	2.78	5.63
C5014(A)-1	11.3	2.48	3.68	6.17	2.45	4.90
C5014(A)-2	10.6	2.25	3.40	5.60	2.39	4.78
C5014(A)-6	9.9	2.03	3.12	5.05	2.00	4.12
C5014(A)-7	9.0	1.76	2.77	4.37	1.92	4.01
C5021(A)-1	15.5	4.01	5.47	9.95	3.59	7.17
C5021(A)-3	13.8	3.36	4.73	8.35	3.43	6.87
C5021(A)-5	12.8	3.00	4.31	7.45	3.29	6.62
C5021(A)-7	11.9	2.68	3.93	6.67	3.19	6.46
C5024(A)-2	12.2	2.79	4.05	6.92	2.89	5.79
C5024(A)-3	12.5	2.89	4.18	7.18	2.76	5.54
C5024(A)-4	12.3	2.82	4.10	7.01	2.65	5.36
C5044 -2	12.9	3.03	4.35	7.54	3.38	6.77
C5044 -5	13.2	3.14	4.47	7.80	2.92	6.00
C50S (A)-1	8.9	1.73	2.73	4.29	1.85	3.70
C50S (A)-2	8.5	1.61	2.58	4.00	1.69	3.43
C50S (A)-3	8.3	1.56	2.51	3.86	1.56	3.22
C4014-3	13.1	3.11	4.43	7.71	3.31	6.64
C4014-7	12.0	2.72	3.97	6.75	2.95	6.01
C4044-2	13.9	3.40	4.77	8.44	4.25	8.50
C4044-3	10.5	2.22	3.36	5.52	4.15	8.31
C4044-E1	13.5	3.25	4.60	8.07	4.00	8.03
C4044-6	11.8	2.65	3.89	6.58	3.87	7.83

classical kinetic theory predicts $R_{p_0} \propto C_0^{0.5} M_0^{1.0}$, and the experimental observation of this relationship has been reported by Cavell[9] in ACV-initiated acrylamide polymerization. As is seen in Figures 4 and 5, the present results agree well with a square root dependence on C_0; however a deviation from first-order dependence of R_{p_0} on M_0 is significant. The least-squares fit for the latter gave $R_{p_0} \propto M_0^{1.24}$. The deviation was further obvious when the conversions of continuous runs were compared for the two runs at the same C_0 level but different M_0. If $R_{p_0} \propto M_0^{1.0}$, the conversion curve should follow the same course regardless of M_0.

In order to explain the observed rate dependence, the classical kinetic theory was modified using the concept of the "cage effect." The following reaction scheme described by North[10] was employed:

Initiation:

$$\mathrm{C} \xrightarrow{k_d} (2\mathrm{R}_c^{\cdot})$$

$$(2\mathrm{R}_c^{\cdot}) \xrightarrow{k_R} \mathrm{Q}$$

$$(2\mathrm{R}_c^{\cdot}) \xrightarrow{k_D} 2\mathrm{R}_c^{\cdot}$$

$$(2\mathrm{R}_c^{\cdot}) + \mathrm{M} \xrightarrow{k_x} \mathrm{R}_1^{\cdot} + \mathrm{R}_c^{\cdot}$$

$$\mathrm{R}_c^{\cdot} + \mathrm{M} \xrightarrow{k_{x'}} \mathrm{R}_1^{\cdot}$$

Propagation:

$$\mathrm{R}_r^{\cdot} + \mathrm{M} \xrightarrow{k_p} \mathrm{R}_{r+1}^{\cdot}$$

Transfer:

$$\mathrm{R}_r + \mathrm{M} \xrightarrow{k_{fm}} \mathrm{P}_r^{\cdot} + \mathrm{M}^{\cdot}$$

$$\mathrm{M}^{\cdot} + \mathrm{M} \xrightarrow{k_{pm}} R_1^{\cdot} \text{ (reinitiation)}$$

Termination:

$$\mathrm{R}_r^{\cdot} + \mathrm{R}_s^{\cdot} \xrightarrow{k_t} \begin{cases} \xrightarrow{k_{td}} \mathrm{P}_r + \mathrm{P}_s \text{ (disproportionation)} \\ \xrightarrow{k_{tc}} \mathrm{P}_{r+s} \quad \text{(recombination)} \end{cases}$$

$$(k_t = k_{tc} + k_{td})$$

Initiator radicals trapped in a solvent cage are denoted by $(2\mathrm{R}_c^{\cdot})$, and Q represents either a waste product or the original initiator molecule.

Water as a solvent has been known to have a chain transfer constant of practically zero.[11] Transfer to the initiator (ACV) was neglected since the degree of polymerization calculated from the intrinsic viscosity was almost independent of the initiator concentration.[9] The termination process is predominantly disproportionation[6,12] and therefore k_t was equated to k_{td} in the following.

Applying the kinetic stationary-state assumption and assuming that the rate constants are independent of chain length, we may write

$$\mathrm{R}^{\cdot} = \left(\frac{2k_d\mathrm{C}}{k_t}\right)^{0.5}\left(\frac{k_\mathrm{D} + k_x\mathrm{M}}{k_\mathrm{R} + k_\mathrm{D} + k_x\mathrm{M}}\right)^{0.5}. \tag{2-a}$$

Assuming $k_\mathrm{D} \ll k_x\mathrm{M}$, which is one extreme case of the two alternative routes that the initiator radical may escape from the cage,

$$\mathrm{R}^{\cdot} = \left(\frac{2k_d\mathrm{C}}{k_t}\right)^{0.5}\left(\frac{\mathrm{M}}{k_\mathrm{R}/k_x + \mathrm{M}}\right)^{0.5}. \tag{2-b}$$

The initiation rate I can be written

$$I = 2k_d\mathrm{C}\left(\frac{\mathrm{M}}{k_\mathrm{R}/k_x + \mathrm{M}}\right) \tag{3a}$$

which is compatible with the conventional expression with the initiator efficiency factor f, $I = 2fk_d\mathrm{C}$, by defining $f = \dfrac{\mathrm{M}}{k_\mathrm{R}/k_x + \mathrm{M}}$. The other extreme case, i.e., $k_\mathrm{D} \gg k_x\mathrm{M}$, leads to the independence of I on M, hence $R_p \propto \mathrm{M}^{1.0}$ which conflicts with our experimental observations.

Now the rate of polymerization can be written

$$R_p = k_p\mathrm{M}\mathrm{R}^{\cdot} = \left(\frac{k_p^2}{k_t}\right)^{0.5}\left(\frac{2k_d\mathrm{C}\mathrm{M}}{k_\mathrm{R}/k_x + \mathrm{M}}\right)^{0.5}\mathrm{M} \tag{4}$$

or in terms of conversion,

$$\frac{dx}{dt} = \left(\frac{k_p^2}{k_t}\right)^{0.5}\left(\frac{2k_d\mathrm{C}\mathrm{M}_0(1-x)}{k_\mathrm{R}/k_x + M_0(1-x)}\right)^{0.5}(1-x). \tag{5}$$

Equation (4) gives $R_{p_0} \propto \mathrm{C}_0^{0.5}\mathrm{M}_0^{1.0\sim1.5}$ depending upon the level of M_0; at high monomer concentration, $R_{p_0} \propto \mathrm{M}_0^{1.0}$, and at low monomer concentration $R_{p_0} \propto \mathrm{M}_0^{1.5}$. Riggs and Rodriguez[4] employed the same expression in explaining $R_{p_0} \propto \mathrm{M}_0^{1.25}$ in the acrylamide polymerization initiated by $\mathrm{K_2S_2O_8}$.

The instantaneous molecular weight distribution of dead polymer being produced at any time t can be written as follows[13]:

$$w(r) = \frac{r}{\bar{r}_n^2}\exp\left(-\frac{r}{r_n}\right) \tag{6}$$

where $\bar{r}_n$ is the instantaneous number-average chain length and is given by

$$\bar{r}_n = \frac{1}{\dfrac{k_t}{k_p^2}\dfrac{R_p}{\mathrm{M}^2} + \dfrac{k_{fm}}{k_p}}. \tag{7}$$

The instantaneous weight-average chain length $\bar{r}_w$ is related to $\bar{r}_n$:

$$\bar{r}_w = 2\,\bar{r}_n.$$

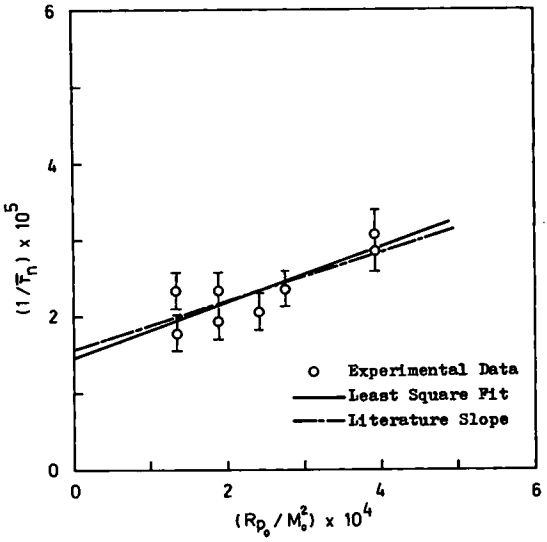

Fig. 6. Plot of $1/\bar{r}_n$ vs. R_{p0}/M_0^2.

The cumulative distribution of dead polymer produced in a conversion interval of $0 \sim x$ can be found by integrating the instantaneous distribution:

$$W(r) = \frac{1}{x}\int_0^x w(r)dx = \frac{1}{x}\int_0^x \frac{r}{\bar{r}_n^2}\exp\left(-\frac{r}{\bar{r}_n}\right)dx. \tag{8}$$

The evaluation of rate constants or groups of rate constants, k_d, k_R/k_x, k_p^2/k_t, and k_{fm}/k_p, follows. Values of these constants are required to predict conversion and molecular weight distribution over a range of conversions and times.

A plot of $1/\bar{r}_n$ versus R_{p0}/M_0^2 was made in Figure 6 using the data of initial rate runs. The first point $\bar{r}_n$ obtained in the continuous runs was included in the figure. From the slope and intercept of the least-squares fitted line (k_p^2/k_t) and (k_{fm}/k_p) were obtained as follows:

	Present experiment	Literature value[2,3]
$\frac{k_p^2}{k_t}$	27.7 (50°C)	31.8 (50°C)[a]
$\frac{k_{fm}}{k_p}$	1.45×10^{-5} (50°C)	1.22×10^{-5} (25°C)

[a] From the value of k_p and k_t at 25°C and their activation energies.

Considering the errors involved in R_{p0} and $\bar{r}_n$, the agreement is reasonable. Since the (k_p^2/k_t) is required to evaluate the initiator decomposition rate k_d, it was decided to use the literature value. This will permit the comparison of our k_d values with those of other workers on the same basis.

Furthermore, the variances in the least-squares fitted line did not show any significant difference from the variance obtained with the best fit line using the slope calculated with the literature value. The latter gave $k_{fm}/k_p = 1.57\times10^{-5}$ (intercept), and this will be used together with the literature value of k_p^2/k_t.

The ratio k_R/k_x may be obtained from two sets of initial polymerization rates $(R_{p_0})_1$ and $(R_{p_0})_2$ measured at two different initial monomer concentrations $(M_0)_1$ and $(M_0)_2$, keeping temperature and the initiator concentration constant:

$$\frac{(R_{p_0})_1}{(R_{p_0})_2} = \left(\frac{k_R/k_x + (M_0)_2}{k_R/k_x + (M_0)_1}\right)^{0.5}\left(\frac{(M_0)_1}{(M_0)_2}\right)^{1.5}$$

$$\therefore \frac{k_R}{k_x} = \frac{(M_0)_2 - \delta(M_0)_1}{\delta - 1}$$

where

$$\delta = \left(\frac{(R_{p_0})_1}{(R_{p_0})_2}\right)^2 \Big/ \left(\frac{(M_0)_1}{(M_0)_2}\right)^3.$$

Once k_R/k_x is obtained, k_d may be calculated using eq. (4). Two sets of initial rate data at 50°C gave the following k_R/k_x and k_d:

Set	k_R/k_x	$k_d \times 10^6$ (l./sec)
I5014–I5024	1.07	3.19
I5024–I5044	0.86	2.87
I5044–I5014	0.96	2.97

The average values of the above are:

$$k_R/k_x = 0.97 \qquad (50°C)$$

$$k_d = 3.00\times10^{-7} \text{ (l./sec)} \qquad (50°C)$$

Applying the same procedure for 40°C data (I4014 and C4044 in which the initial conversion data were used to obtain R_{p_0}), the following values were obtained:

$$k_R/k_x = 1.20 \qquad (40°C)$$

$$k_d = 7.20\times10^{-7} \text{ (l./sec)} \qquad (40°C)$$

For 25°C and 30°C data, the term $f\cdot k_d = \left(\frac{M_0}{k_R/k_x + M_0}\right) k_d$ was evaluated and values are tabulated in Table II.

Comparison of k_d or $f\cdot k_d$ values are made in Figure 7 with those reported in the literature. The solid line represents k_d based on the present data at 40°C and 50°C:

$$k_d = 7.70\times10^{13} \exp(-28.7\times10^3/RT).$$

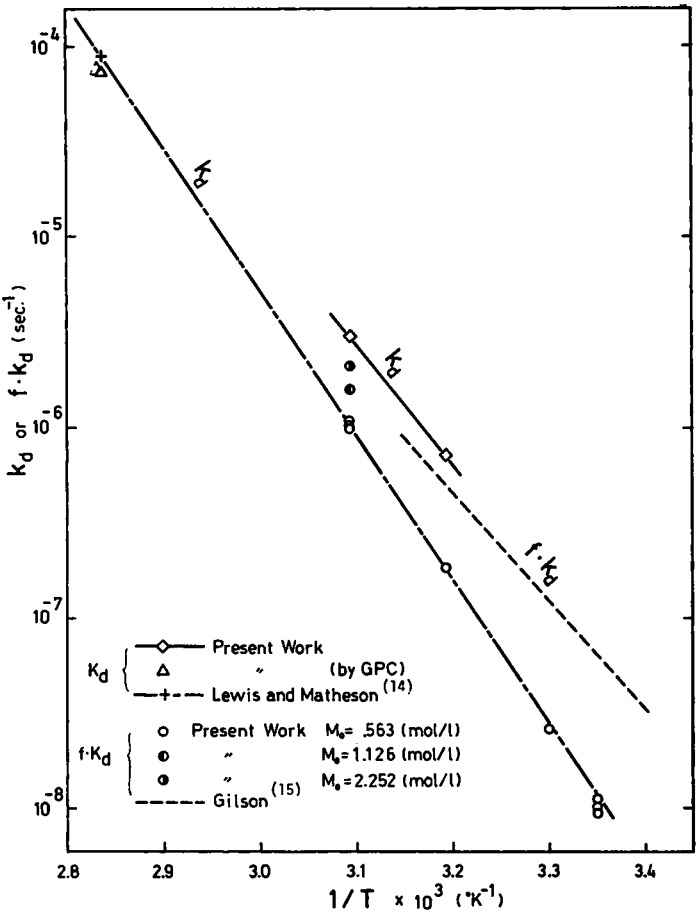

Fig. 7. Comparison of $k_d(f \cdot k_d)$.

Lewis and Matheson[14] have reported $k_d = 8.97 \times 10^{-5}$ (1/sec) at 80°C together with the activation energy of 34.0 (kcal/mole). These were obtained using a measurement of nitrogen evolution; however, their temperature range of the measurement is not reported. The (— - — -) line represents their k_d values calculated using the activation energy, while the dotted line represents $f \cdot k_d$ values obtained by measuring the rate of acrylamide polymerization.[15] Present $f \cdot k_d$ values at $M_0 = 0.563$ (mole/l.) are in reasonable agreement with Lewis and Matheson's k_d. However, at higher monomer concentrations, the values of $f \cdot k_d$ exceeded their k_d values showing an apparent contradiction with $f > 1.0$. The same contradiction occurred when Gilson compared his $f \cdot k_d$ values with Lewis and Matheson's k_d. The present k_d data are reasonable in that initiator efficiencies are less than unity for Gilson's $f \cdot k_d$ values as well as for the present values.

The decomposition of ACV was therefore followed using GPC to obtain and compare k_d value at 80°C. The change of GPC elution chromato-

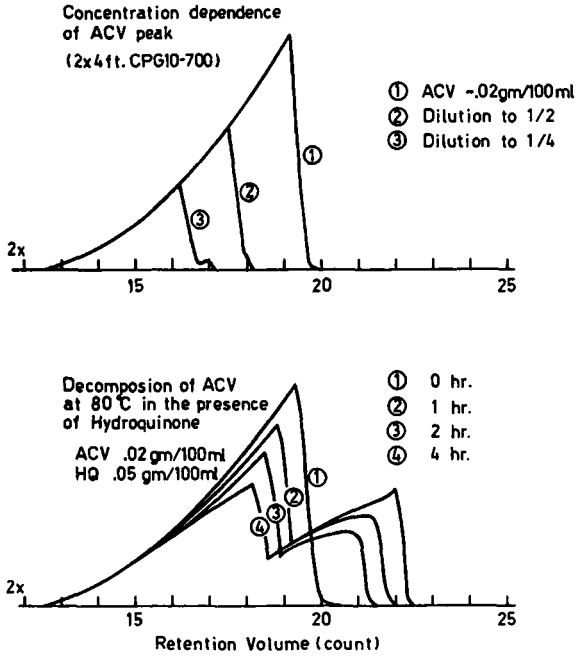

Fig. 8. GPC response for ACV.

grams for the ACV solution with the presence of hydroquinone is shown in Figure 8. Under the assumption that the leading peak represents remaining ACV fraction, the decomposition rate constant was evaluated as 7.5×10^{-5} (1/sec) from the slope of initial decrease of C/C_0, giving k_d slightly lower than Lewis and Matheson's value. Since k_d thus estimated could possibly be lower than the true value due to imperfect separation of the ACV peak from the decomposed materials which may lead to overestimation of C, the reported value at 80°C appears reasonable.

Comparison of Measured and Predicted Quantities

The initiator decomposition rate constant k_d and the rate constant groups k_R/k_x, k_p^2/k_t, and k_{fm}/k_p described in the above were used to calculate the variation of conversion and molecular weight distribution with time. Both quantities were obtained by numerical integration. The step size Δt for the calculation was always adjusted so that the conversion increase Δx in the time increment was less than 1%. This step size was found sufficient to satisfy an obvious relationship $\bar{P}_n[P] = M_0x$ within 1% error, where $\bar{P}_n$ is the number-average degree of polymerization (cumulative) and [P] is cumulative dead polymer concentration.

In Figures 9 to 14, the present experimental values of conversion and number-average molecular weights at 50°C are compared with those predicted. Comparison of weight-average molecular weights is made in Figure 15, in which two different equations relating intrinsic viscosity- to weight-average molecular weight are employed.

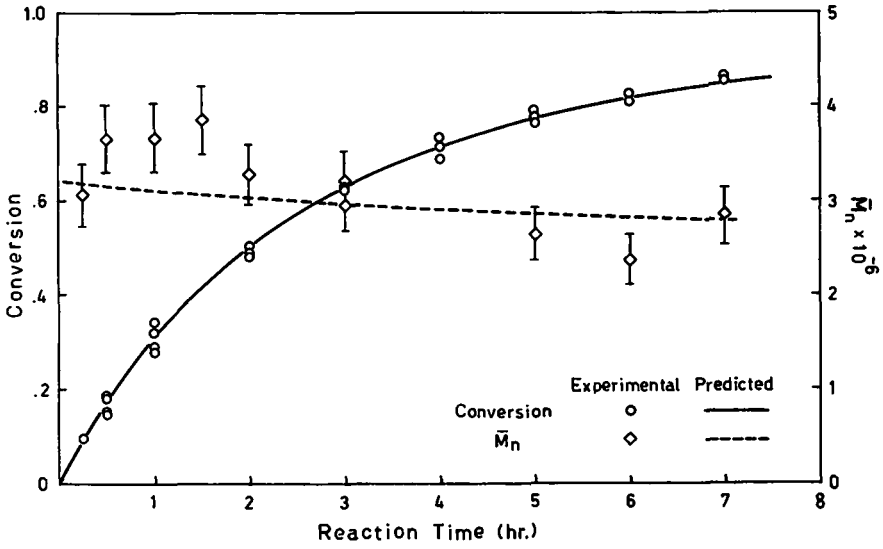

Fig. 9. Comparison of conversion and $\bar{M}_n$: runs I5011, C5011(A)-(D).

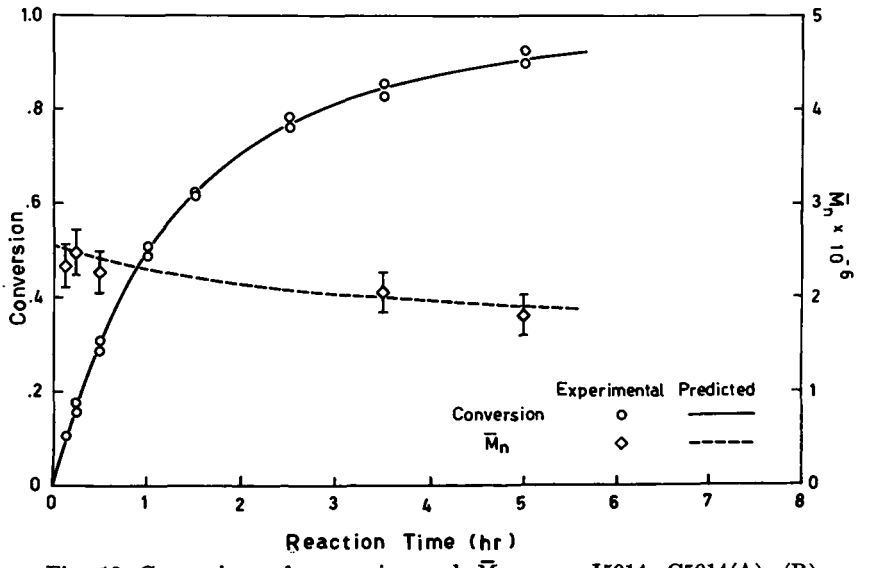

Fig. 10. Comparison of conversion and $\bar{M}_n$: runs I5014, C5014(A), (B).

Figure 16 shows examples of electron micrographs of polyacrylamide molecules. Polystyrene molecules mixed with polyacrylamide as a calibration standard (diameter 0.264 μ; Dow Chemical) appeared as a well-formed sphere while smaller polyacrylamide molecules were distorted to some extent. The shadow lengths of more than 500 well-isolated polyacrylamide molecules were measured by TGZ3 particle size analyzer (Carl Zeiss) after the magnification of the original micrographs from ~4×4~×80,000. Molecular diameters were calculated using the average

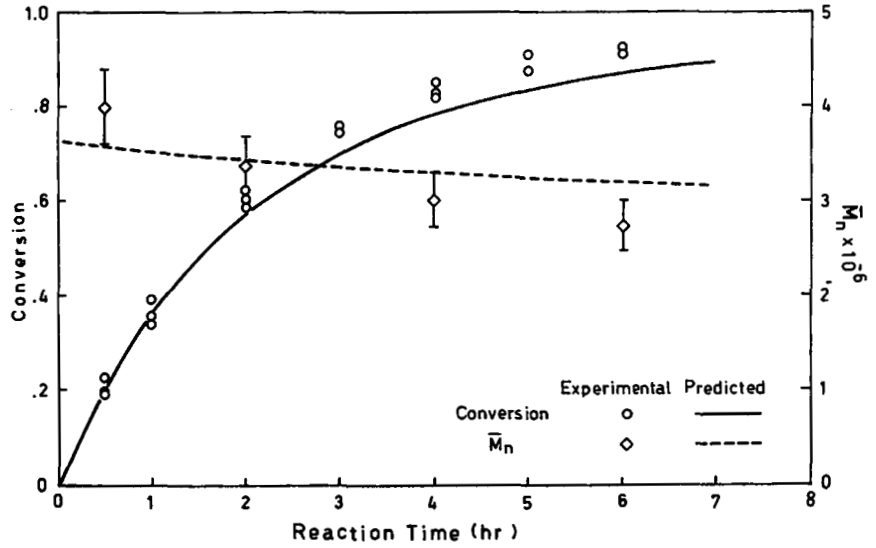

Fig. 11. Comparison of conversion and $\bar{M}_n$: runs C5021(A), (B).

shadow length of polystyrene molecules and converted into a molecular weight distribution shown in Figure 17. The density of single molecules was estimated using $\bar{M}_n$ obtained by viscometry and setting this equal to $\bar{M}_n$ by electron microscopy. This gave $\bar{M}_n = 2.86 \times 10^6$ and $\bar{M}_w = 5.95 \times 10^6$.

The refractive index increment of polyacrylamide solution was found to be 0.161 (ml/g) (Brice-Phoenix differential refractometer, 546 mμ). This

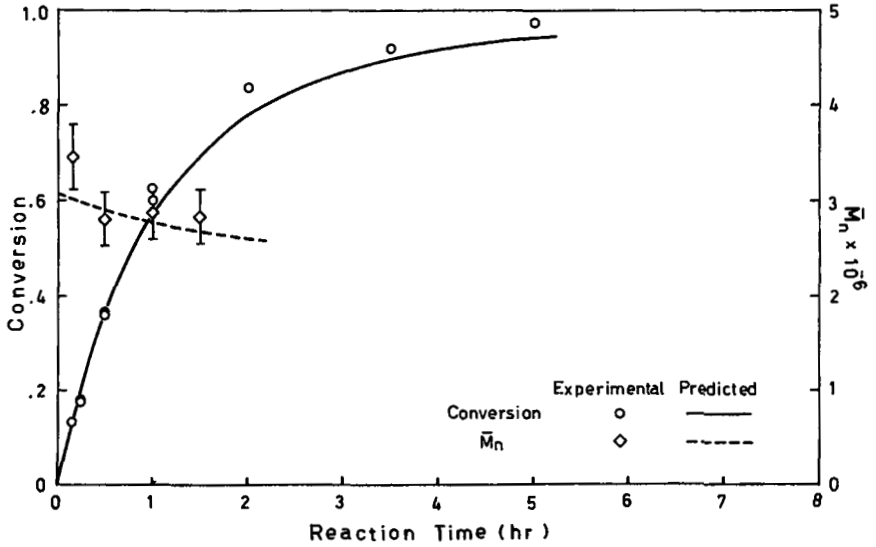

Fig. 12. Comparison of conversion and $\bar{M}_w$: runs I5024, C5024(A), (B).

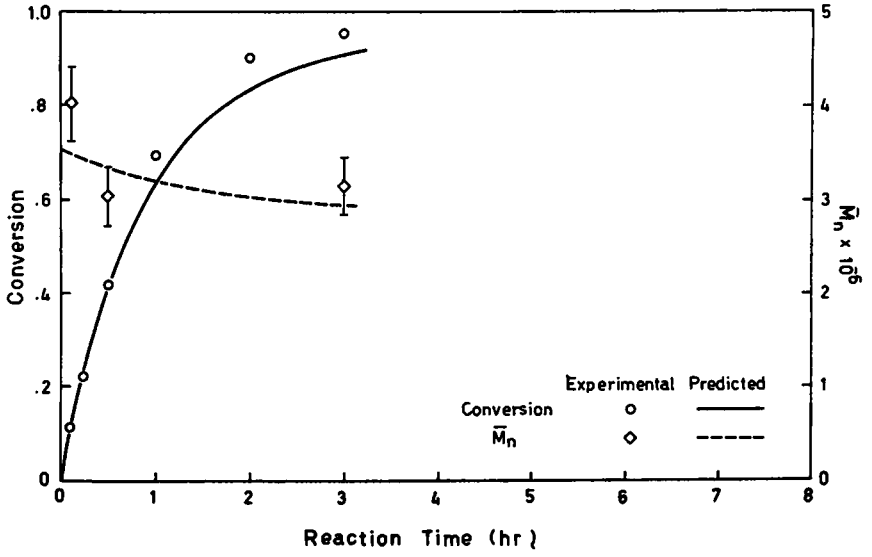

Fig. 13. Comparison of conversion and $\bar{M}_n$: runs I5044, C5044.

compares to the reported values of 0.163[8] and 0.186.[16] Using the present value, a Zimm plot was made in Figure 18 for the same polyacrylamide sample as was used with electron microscopy. The extrapolation of Kc/R_θ to zero angle and zero concentration yielded $\bar{M}_w = 6.3 \times 10^6$.

GPC responses for two polymer samples are shown in Figures 19 and 20. A linear effective calibration curve[17] that gave the best fit for the $\bar{M}_n$ values of the two samples (by viscometry) was searched and used to convert the chromatograms from retention volume scale to molecular weight scale.

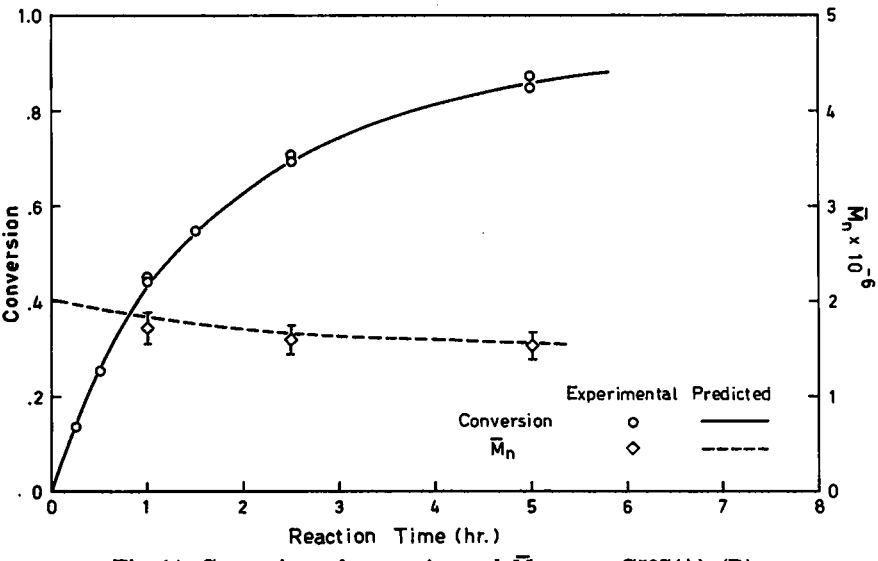

Fig. 14. Comparison of conversion and $\bar{M}_n$: runs C50S(A), (B).

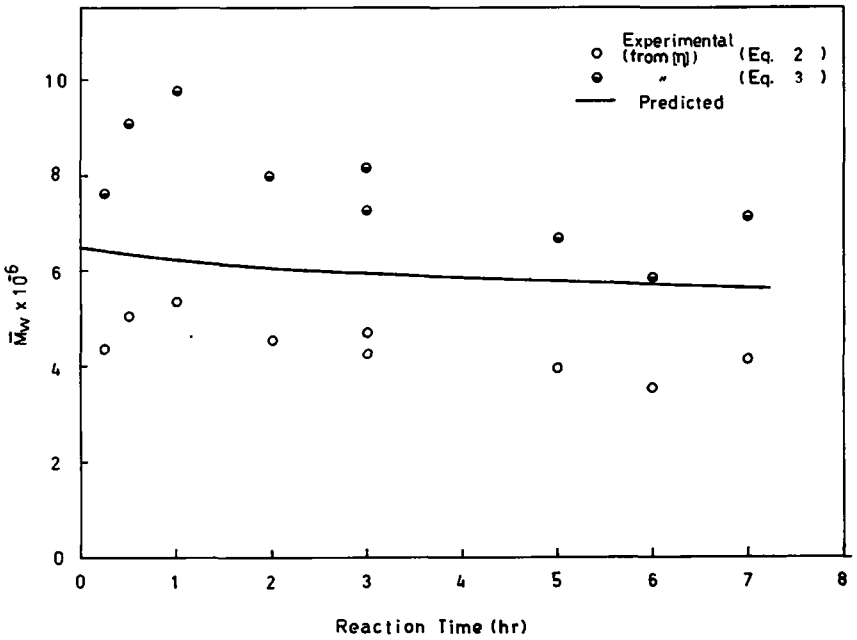

Fig. 15. Comparison of $\bar{M}_w$: runs C5011(A), (B).

DISCUSSION

Observed rate dependence of $R_{p_0} \propto C_0^{0.5}M_0^{1.24}$ in ACV-initiated polymerization agrees well with the previously reported work in regard to the exponent of the initiator concentration but differs in the exponent of the monomer concentration. The present data agree better with polymerizations initiated with potassium persulfate and other chemical initiators where the monomer dependence of R_{p_0} was always greater than unity. Also the initiator ACV when employed in styrene polymerization[18] showed a monomer dependence greater than unity. From this view, the present results are not unexpected, but the disagreement with Cavel and Gilson's[9,15] work is difficult to explain. In terms of ACV decomposition rate constant k_d, the present results are not in disagreement with their results. The decomposition rate constant of ACV was significantly higher than the one based on measurements of nitrogen evolution at 80°C.[14] Since reasonable agreement of k_d at 80°C is obtained in different experiments, the activation energy quoted[14] for ACV decomposition may be a little too large.

The kinetic scheme describing the dependence of initiation rate on monomer concentration well explains the observed rate dependence. The choice of cage effect to explain the results may be more reasonable than complex theory. If one uses the complex theory, the evaluated equilibrium constant $K_e\left(=\left(\frac{k_R}{k_x}\right)^{-1}\right)$ for the complex shows a larger value at 50°C than at 40°C, and again this is the reason why the cage effect theory is generally preferred over the complex theory.

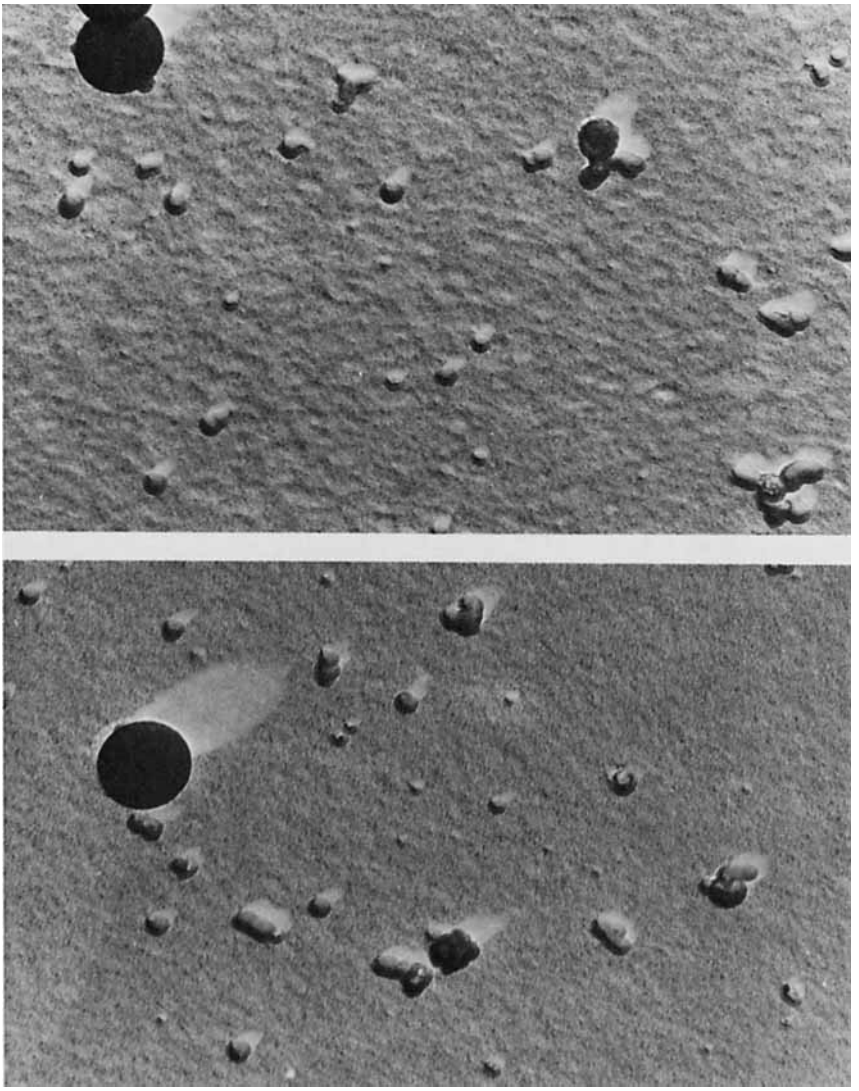

Fig. 16. Examples of micrographs [original (~×20,000) × 1.5].

The groups of rate constants k_p^2/k_t and k_{fm}/k_p evaluated from the initial rate and number-average molecular weight data showed reasonable agreement with reported data. Use of the literature values of k_p^2/k_t can be justified since the difference from the present value is not significant. The use of literature values permits a comparison of initiator decomposition constants found by various workers on a common basis.

Agreement in both conversion and number-average molecular weight between measured and predicted were very satisfactory for monomer concentrations less than 0.563 (mole/l.). Previously it was indicated that a single kinetic scheme was valid to 80–90% conversion when the product

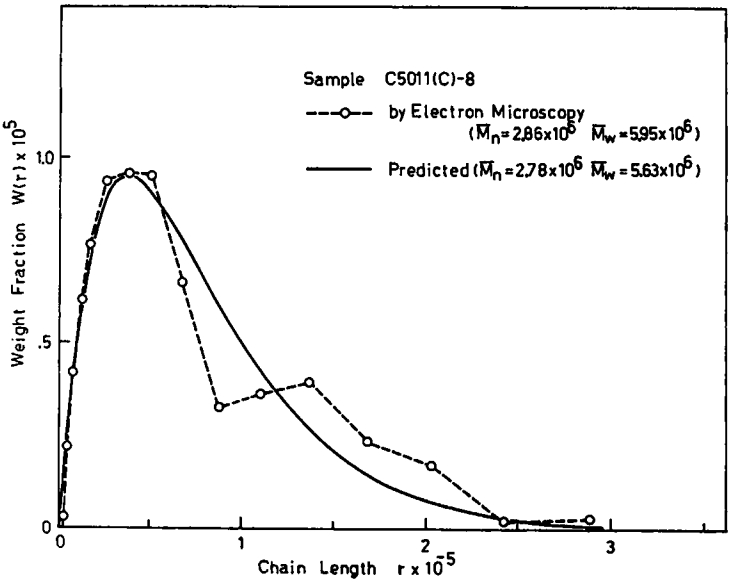

Fig. 17. Comparison of molecular weight distribution.

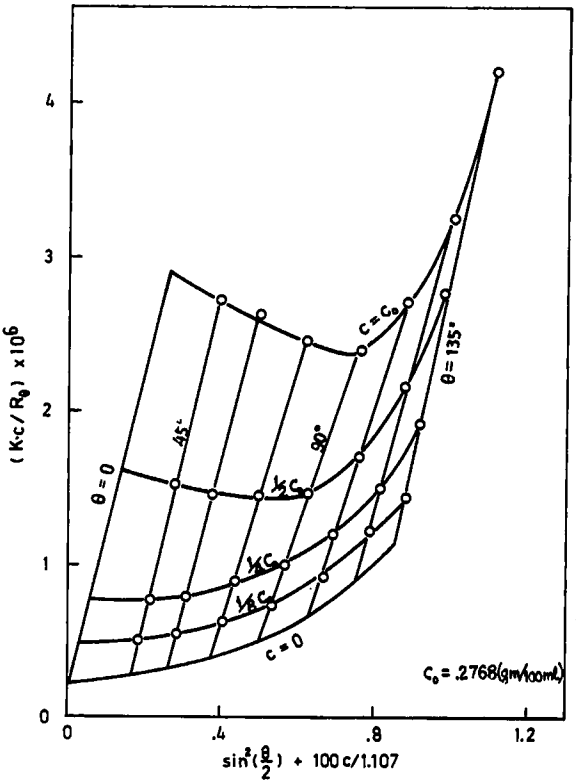

Fig. 18. Zimm plot for sample C5011(C)-8.

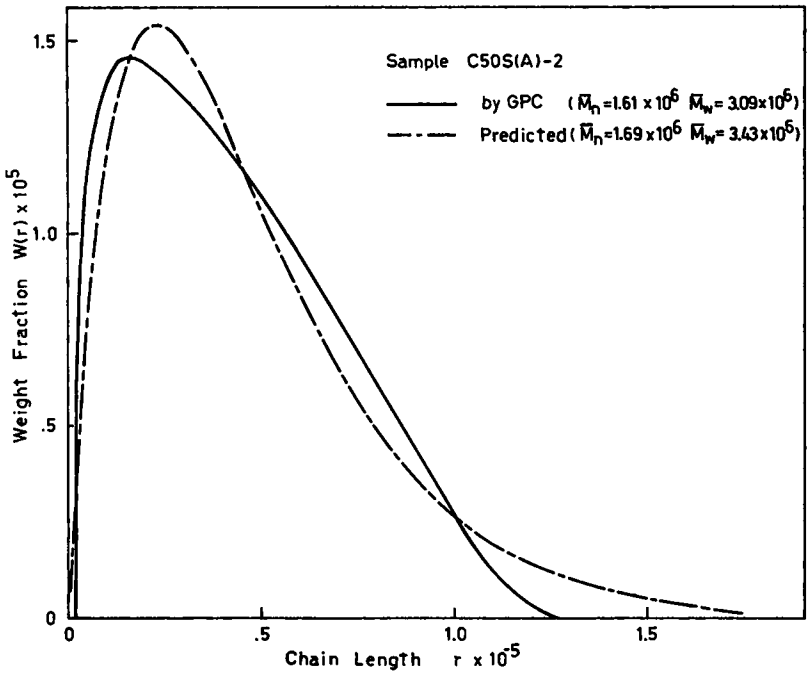

Fig. 19. Comparison of molecular weight distribution.

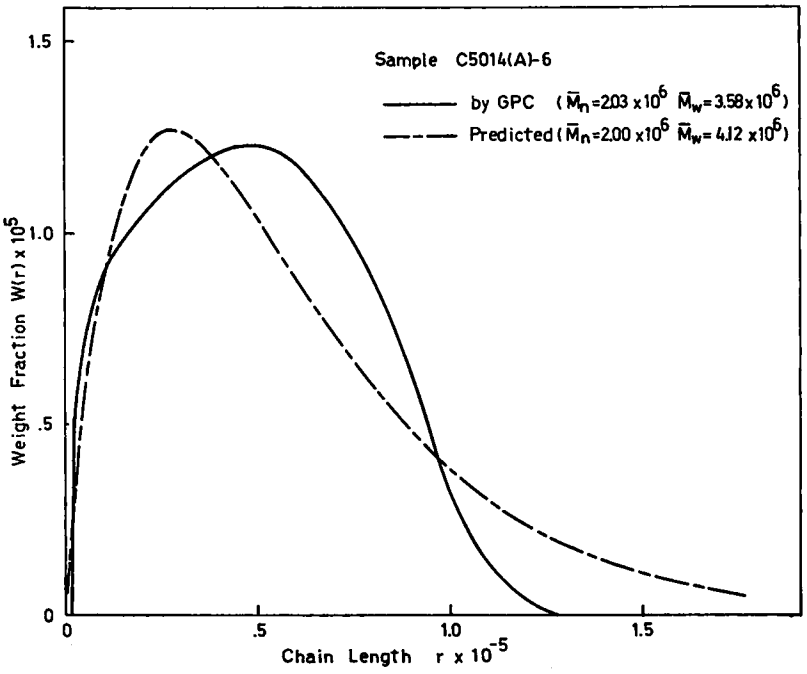

Fig. 20. Comparison of molecular weight distribution.

polymer is in the order of 10^5 in molecular weight.[4,6] The present results extend this range of applicability to 10^6 when the monomer concentration is relatively low. At initial monomer concentrations of 1.126 or 2.252 (mole/l.), the experimental conversion data were always greater than the predicted ones at conversion over 40%. The maximum difference was ~10% in conversion at 50°C, while it was ~15% at 40°C. Measured conversion values in viscous media (usually at high conversions) are generally greater than predicted ones for vinyl free-radical polymerization. These deviations are usually explained in terms of diffusion control of the termination reaction (gel effect). With the assumption that the difference in the present results is due to the variation of k_p^2/k_t with increasing conversion, the change of k_p^2/k_t was estimated from experimental conversion curves using eq. (5). The decrease of k_p^2/k_t as compared to its initial value was found much smaller than that reported for styrene polymerization in toluene. It appears that the gel effect is of very minor importance in acrylamide polymerization.

As far as the number-average molecular weight is concerned, the agreement between measured and predicted ones was satisfactory at all conversions. As is indicated by eq. (7), $\bar{r}_n$ is predominantly controlled by the term k_{fm}/k_p when molecular weights of order of 10^6 are being produced. When one employs fast initiation systems (large R_p) or low monomer concentrations, the term $(k_t/k_p^2)(R_p/\mathrm{M}^2)$ may control $\bar{r}_n$ rather than k_{fm}/k_p, resulting in a smaller molecular weight product and the possibility of molecular weights being influenced by the gel effect. At a temperature 25°C, k_{fm}/k_p exceeds $(k_t/k_p^2)(R_p/\mathrm{M}^2)$ by nearly ten times, leaving $\bar{M}_n$ virtually constant as was observed. This could also explain the results of Cavell,[9] who obtained almost constant values for the average molecular weights when changing the initiator concentration level by tenfold. In the present higher monomer concentration runs, the deviation of measured conversion from that expected by the kinetic scheme was observed. This is an indication of a possible gel effect.

The predicted weight-average molecular weights fell in between those calculated from the intrinsic viscosity values. However, the difference in values based on the two empirical correlations is too large to be useful in testing the validity of the kinetic model. On the other hand, weight-average molecular weight measured by light scattering and by electron-microscopy have a polydispersity of the sample of 2.2 and 2.1, respectively. This is in reasonable agreement with theoretical kinetics which gives a polydispersity of 2.0.

Molecular weight distribution analysis by GPC suffered from lack of column resolution for the high molecular weight tail. Molecules above certain molecular weight elute like smaller molecules, and thus the tailing portion of the molecular weight distribution was not detected. However, the electron microscopy clearly shows the existence of the large molecular weight tail. As opposed to GPC, electron microscopy has a certain lower molecular weight limit for the detection of an individual molecule, but in the

molecular weight range of a few million, it does not suffer from this limit. Advantage of this technique for molecular weight distribution analysis of polyacrylamide has been shown by Wade and Kumar[20] in shear degradation study of polyacrylamide solution.

CONCLUSIONS

Experimental investigation was made on polymerization of acrylamide in water with ACV in such conditions that the product polymer had a number-average molecular weight over one million.

Initial rate of polymerization showed a monomer dependence of greater than unity, thus the classical kinetic theory was modified according to "cage effect." The evaluated rate constants k_p^2/k_t and k_{fm}/k_p showed reasonable agreement with those reported. The decomposition rate constant k_d of ACV, however, was larger than that expected from the reported k_d at 80°C and the activation energy.

Prediction of conversion and molecular weight variations with respect to reaction time were made using the proposed kinetic scheme. The predicted values agreed well with those measured indicating the validity of the kinetic model to high conversion when initial monomer concentration is less than 0.56 (mole/l.). At the initial monomer concentration 1.12 and 2.25 (mole/l.), the predicted conversions were always lower than the measured ones at high conversion, indicating possible "gel effect." Predicted number-average molecular weight however was in reasonable agreement with the measured one at all levels of the monomer concentration. This is due to the fact that transfer to monomer is dominant in controlling the molecular weight when the molecular weight is as high as a few million. For this reason, the gel effect does not affect the molecular weight of the polymer.

Weight-average molecular weight obtained by light scattering and molecular weight distribution obtained by electron microscopy give further support for the validity of the kinetic scheme.

The authors wish to acknowledge financial support received from Nalco Chemical Co., Chicago (USA), and the National Research Council of Canada and the receipt of a fellowship by one of us (T. Ishige) from McMaster University.

Nomenclature

ACV	4,4-azobis-4-cyanovaleric acid
c	polymer concentration
C	initiator and its concentration
C_0	initial initiator concentration
f	initiator efficiency
HQ	hydroquinone
I	initiation rate
k	rate constant
K	angular constant

Ke	equilibrium constant
M	monomer and its concentration
M_0	initial monomer concentration
$M\cdot$	monomer radical
$\bar{M}_n$, $\bar{M}_w$	number- and weight-average molecular weight
[P]	total polymer concentration
$\bar{P}_n$	number-average degree of polymerization (cumulative)
Q	waste product or original intiator
r	chain length
$\bar{r}_n$, $\bar{r}_w$	number- and weight-average chain length (instantaneous)
$R\cdot$	total radical concentration
$R_c\cdot$	decomposed initiator radical and its concentration
$R_r\cdot$	radical with chain length r and its concentration
R_p	rate of polymerization
R_{p_0}	initial rate of polymerization
R_θ	Rayleigh ratio
t, Δt	time
$w(r)$	molecular weight distribution with respect to chain length (instantaneous)
$W(r)$	molecular weight distribution with respect to chain length (cumulative)
x, Δx	conversion
δ	a constant
$[\eta]$	intrinsic viscosity
θ	observation angle

Appendix I

$\bar{M}_n$ and $\bar{M}_w$ Measurements by Viscometry and Light Scattering

Viscometry

Solution viscosity of polyacrylamide in water was measured at 25°C using a Cannon-Ubbelhode viscometer 50-A620. Polyacrylamide was dissolved in distilled water at 50°C over a 24-hr period. The polymer concentration was about 0.1 g/100 ml of solution. The solutions were then filtered through a 50-micron sintered glass filter. Successive dilution in the viscometer was made giving about 0.02 g/100 ml. Efflux times ranged from 4 to 10 min, and it was thus felt that a kinetic energy correction was unnecessary. Within the concentration range studied, a linear relationship between η_{sp}/c versus c was observed, and intrinsic viscosities were obtained by extrapolating to zero concentration. Number-average molecular weight was calculated using eq. (1), which was obtained using number-average molecular weights up to 2×10^5. This equation was used in the present study for number-average molecular weights up to 5×10^6. Equation (1) has also been used at number-average molecular weights greater than 2×10^5 by Dainton et al.[1] and Suen et al.[21] In the former investigation, no conclusions were made about its validity at higher molecular weights, while in the latter investigation, the estimated k_p^2/k_t obtained using eq. (1) showed reasonable agreement with that reported by Dainton et al.,[1] indicating that it may be valid for number-average molecular weights appreciably greater than 2×10^5.

Light Scattering

Intensities of scattered light from polyacrylamide solutions (solvent: distilled water) were measured with a Brice Phoenix Universal light-scattering photometer at room temperature. The wavelength employed was 546 mμ. The solution was prepared in the same manner as with viscosity measurements. Initial concentration of the polyacrylamide solution was 0.2768 g/100 ml, and this was diluted by $^1/_2$, $^1/_4$ and $^1/_8$. Solvent was filtered with 0.22-micron Millipore filter, while the solution was filtered with 1.2-micron Millipore filter under pressure. Attempts to filter the solution with a 0.22-micron filter was not possible.

Separate measurements of the refractive index increment of polyacrylamide solutions were made with a differential refractometer (Brice Phoenix). The dn/dc obtained was 0.161 (ml/g). This compares with reported values of 0.163[22] and 0.186.[8]

$\bar{M}_w$ obtained for the sample was 6.3×10^6. By assuming a polydispersity of 2.0, $\bar{M}_n$ should be $\sim3.15\times10^6$. This may be compared with $\bar{M}_n = 2.86\times10^6$ obtained by viscometry with the use of eq. (1). It appears that eq. (1) can be used for polyacrylamide with a number-average molecular weight as large as 3×10^6. Further evidence for this validity was obtained with a measurement of the molecular weight distribution by electron microscopy.

Appendix II

MWD Analysis by Electron Microscopy

Specimen preparation followed the procedure developed by Wade and Kumar.[20] To a polyacrylamide solution of 40 wppm in distilled water was slowly added a non-solvent, *n*-propanol, to give a theta solvent of 20% water and 80% *n*-propanol. Polystyrene latex (Dow Chemical) of particle diameter 0.264 micron was added to these solutions as a calibration standard. Then the solutions were sprayed onto a copper substrate, shadowed with gold–palladium, and protected by carbon.

Micrographs were obtained at a magnification of $\sim\times20{,}000$. Shadow lengths of well-isolated molecules (more than 500) were measured with a particle size analyzer TGZ3 (Carl Zeiss) after magnification of the micrographs $\sim\times4$. Polystyrene and polyacrylamide molecules were assumed to be spherical, and their effective diameters were calculated from shadow lengths.

Number- and weight-average molecular weights are related to number fraction $f(r)$ with molecular diameter r in the following manner:

$$\bar{M}_n = \frac{4}{3}\pi\rho N\int_0^\infty r^3 f(r)dr$$

$$\bar{M}_w = \frac{4}{3}\pi\rho N\int_0^\infty r^6 f(r)dr \Big/ \int_0^\infty r^3 f(r)dr.$$

The above integral was evaluated using Simpson's rule. The molecular density ρ was obtained by equating the above $\bar{M}_n$ with the one obtained by viscometry. The density ρ thus obtained was 0.89 (g/cm^3), as compared to the density of monomer 1.122 (g/cm^3). If one assumes that the density of polyacrylamide spheres is equal to the density of acrylamide monomer, both $\bar{M}_n$ and $\bar{M}_w$ would be raised by about 20%.

In reporting MWD (in Figs. 17, 19, and 20), the molecular weight scale was represented by chain length using the monomer molecular weight of 71.08. In calculating polydispersity the particle density cancels out.

Appendix III

Conversion and MWD Analysis by GPC

The GPC employed in this experiment was Waters' ALC Model 201, and it was operated at room temperature. The injection septum was replaced with an injection valve having a 1-ml sample loop. Conversion analysis was made with single 4-ft (O.D. $^3/_8$ in. stainless steel) column packed with CPG 10-700 (Waters). Distilled water was used as the carrier solvent. Separation of polymer from monomer was found adequate with a single column. Operation with a single column gave a stable baseline and short analysis time (30 min/run).

For molecular weight analysis, the following combination of six 4-ft columns was used: 2×(Bio-Glass 2500) + 3×(CPG 10-2000) + 1×(CPG 10-700). The carrier solvent water contained 0.15 wt-% KBr as buffer. This eliminated the effect of polymer concentration on retention volume. The polymer concentration range used was 0.05 0.10 wt-%. At higher polymer concentrations, linearity between polymer concentration and chromatogram heights was not observed.

An effective linear calibration curve[17] was found using two number-average molecular weights obtained by viscometry. This effective linear molecular weight calibration curve was then used to convert the GPC response to a differential molecular weight distribution.

References

1. E. Collinson, F. S. Dainton, and G. S. McNaughton, *Trans. Faraday Soc.*, **53**, 476' 489 (1957).
2. F. S. Dainton and M. Tordoff, *ibid.*, **53**, 499, 666 (1957).
3. E. Collinson, F. S. Dainton, D. R. Smith, G. J. Trudel, and S. Tazuke, *Discuss. Faraday Soc.*, **29**, 188 (1960).
4. J. P. Riggs and F. Rodriguez, *J. Polym. Sci. A-1*, **5**, 3151 (1967).
5. J. P. Friend and A. E. Alexander, *ibid.*, **6**, 1833 (1968).
6. K. Venketarao and M. Santappa, *ibid.*, **8**, 1785 (1970).
7. W. Scholtan, *Makromol. Chem.*, **14**, 169 (1954).
8. Technical Bulletin, *Cyanamer Polyacrylamide*, American Cyanamide Co., Wayne, N.J., 1967.
9. E. A. S. Cavell, *Makromol. Chem.*, **54**, 70 (1962).
10. A. M. North, *The Kinetics of Free Radical Polymerization*, Pergamon Press, New York, 1966.
11. F. S. Dainton, *J. Chem. Soc.*, 1533 (1952).
12. T. J. Suen and D. F. Rossler, *J. Appl. Polym. Sci.*, **3**(7), 126 (1960).
13. A. E. Hamielec, in Symposium on Polymer Reactor Engineering, Quebec City, June, 1972.
14. E. M. Lewis and M. S. Matheson, *J. Amer. Chem. Soc.*, **71**, 747 (1949).
15. I. T. Gilson, Ph.D. Thesis, University of Southampton, 1963.
16. H. J. Cantow, *Z. Naturforsch.*, **7b**, 485 (1952).
17. S. T. Balke, A. E. Hamielec, and B. P. LeClair, *Ind. Eng. Chem., Prod. Res. Develop.*, **8**, 54 (1969).
18. G. S. Misra, R. C. Rastogi, and V. P. Gupta, *Makromol. Chem.*, **50**, 72 (1961).
19. M. Harada, T. Yamada, K. Tanaka, W. Eguchi, and S. Nagata, *Kagaku Kogaku*, **29**, 301 (1965).
20. J. H. T. Wade and P. Kumar, *J. Hydronautics*, **6**, 41 (1962).
21. T. J. Suen, Y. Jen, and J. V. Lockwood, *J. Polym. Sci.*, **31**, 481 (1958).
22. H. J. Cantow, *Z. Naturforsch.*, **7B**, 485 (1952).

Received June 19, 1972
Revised October 6, 1972